

Coastal Areas Noise Floor Characterization in 2.4GHz ISM Band

Rayan Enaya, Ivica Kostanic and Josko Zec

CSE Department of Florida Institute of Technology, Melbourne, FL, USA

ABSTRACT

The noise-rise in the 2.4GHz ISM band over coastal waters is considered. The characterization of the noise is performed using spectrum scan measurements of the band. It was established that the most dominant source of the noise is the Wi-Fi deployment on the land. A model for the noise prediction that is based on population density is developed. The model is calibrated using a set of measurements. The performance of the model is evaluated using an independent set of measurements (i.e., a set that was not used for calibration). The difference between noise measurements and predictions is on average smaller than 3dB and with standard deviation on the order of 2.9dB.

Keywords - . Noise floor modeling, radio communication in coastal waters.

Date of Submission: 07-02-2021

Date of Acceptance: 21-02-2021

I. INTRODUCTION

In the modern world, wireless communication represents an important part of one's day-to-day life. Through a cellphone, a laptop, and other wireless devices one keeps in touch with the work and social circles, conduct his or her personal business and gets access to entertainment. However, there are still few places where the wireless connectivity is not readily available. An example of such places are coastal waters. While being on land, users may rely on terrestrial networks, like cellular or Wi-Fi, to obtain connectivity. On large boats, which are traveling through deeper waters (e.g., more than 10 miles away from the shore), the connectivity may be obtained through satellite Internet providers. For larger boats, the size of the satellite equipment does not present a problem. Also, even though satellite services are expensive, the costs are negligible when compared with the overall operational costs of a larger boat. However, in coastal waters, the situation is much different. The boats in the coastal waters are smaller boats which cannot carry the satellite equipment easily. At the same time, the coverage obtained from terrestrial (mostly cellular) networks is often accidental. The quality of such connectivity is usually very poor. As a result, for smaller boats operating near the shore, there is no viable solution for obtaining a reliable Internet data connectivity.

In [1], a case is advanced for a terrestrial network specifically designed for providing coverage to wireless devices in coastal waters. It is proposed that the network operates in 2.4GHz ISM band (2400-2483.5MHz). As a first step towards this goal, [1] documents a series of propagation

studies in the coastal areas and for the 2.4GHz ISM band. The path loss model is developed, and its accuracy is assessed.

The 2.4GHz ISM band is unlicensed, and therefore, it is shared by many wireless technologies. The band is regulated by CFR Title 47, Chapter I, FCC Part 15 [2]. Devices currently operating in this band are numerous and they create a substantial radio noise that needs to be tolerated by every upcoming new technology. It is the aim of this paper to characterize this noise as it exists within the coastal waters.

The outline of the paper is provided as follows. Section 2 describes used noise floor measurement equipment and the data collection process. The analysis of the measurements is presented in Section 3. Section 4 presents a model that allows prediction of the noise floor characteristics in the vicinity of the shore. The model is calibrated using measured data. Also, a model validation on an independent data set is performed. Finally, some summary observations and conclusions are provided in Section 5.

II. DATA COLLECTION SETUP AND MEASUREMENTS

The characterization of 2.4GHz noise floor is conducted on the basis of measurements. The overall setup of the data collection equipment is presented in Figs. 1 (a) and 1 (b). The setup is very simple. The spectrum scanner in Fig. 1(a) is a commercial receiver made by PCTEL – Seagull [3]. The signal is received by an omnidirectional 2.4GHz antenna with the gain of 0dBi. The antenna is elevated on a ladder so that there is no blockage from other objects on the deck of the boat. The

antenna is at the height of about 3m above the surface of the ocean. Seagull has a built in GPS receiver which stamps each spectrum measurement with a geo location and time. Finally, the receiver is connected to a laptop which runs the software for automated collection of the measurements.

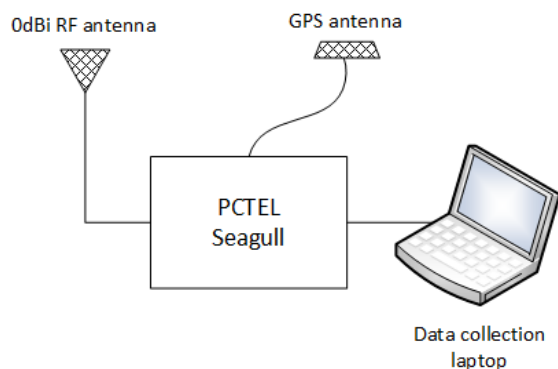


Figure 1 (a). Schematic of data collection equipment

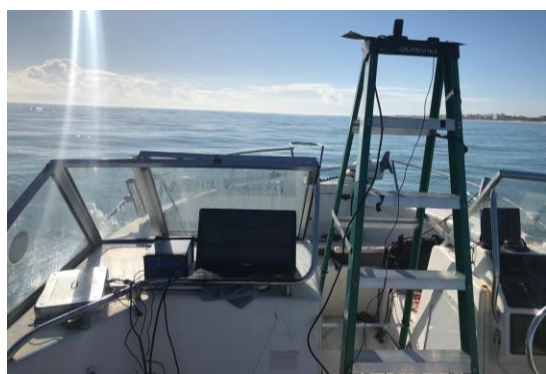


Figure 1 (b). Picture of the equipment setup on the boat

The receiver is set up to perform a spectrum scan of the 2.4GHz band in accordance with parameters given in Table 1. There are 2088 scanned frequencies across the band. The frequencies are separated by 40kHz and the front-end filter bandwidth used for the scan is 80kHz. The noise figure of the receiver is 5dB, so the noise floor is at -120dBm. An example of a spectrum scan obtained by the equipment is presented in Fig. 2. One sees that there are some portions of the spectrum that are quiet, and the Rx Power is about -120dBm. However, there are portions of the spectrum where the received power is as high as -97dBm. This indicates a noise rise of 23dB.

Table 1. Parameters of the scanning receiver

Parameter	Value	Unit
Start frequency	2400	MHz
End frequency	2483.5	MHz

Frequency increment	40	kHz
Bandwidth (B)	80	kHz
Number of frequencies across the band	2088	
Noise figure of the receiver (F)	5	dB
Noise floor in 80kHz $10 \log(kTB) + F$ [dB]	-120	dBm

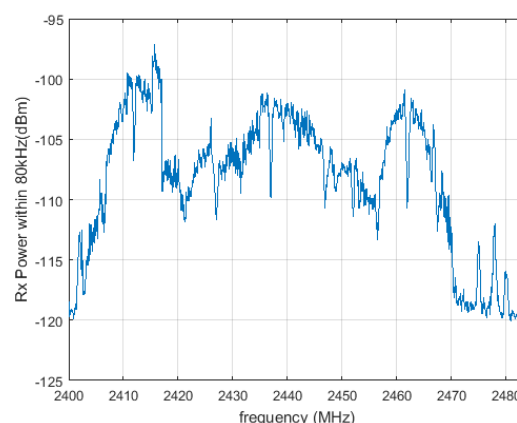
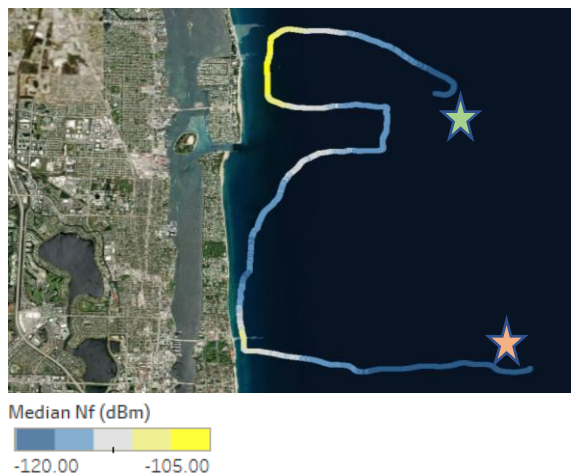


Figure 2. An example spectrum scan of the 2.4GHz ISM band

As an illustration, a trajectory of the boat during data collection is presented in Fig. 3. The measurements were collected along the coast of West Palm Beach, FL, USA. The area is an example of a populated urban area along Florida's coasts. A significant noise rise in the ISM band is expected. This is indeed the case. From Fig. 3 one sees that as the boat operates close to the shore, the median noise power within 80kHz becomes as high as -95dBm. This corresponds to a noise rise that is on the order 25dB. However, as the boat travels further from the shore, the power of the noise decreases fairly quickly.

III. DATA ANALYSIS

A spectrogram produced from all measurements in Fig. 3 is presented in Fig 4. The frequency range used for data collection is plotted along the x-axis. Each row of the image in Fig. 4 represents a single spectrum scan (like the one shown in Fig. 2.).



The color of the trace indicates median noise power across the band. The power is measured within a bandwidth of 80 kHz. (c.f. Table 1). The collection starts at the “green star” and ends at the “red star”.

Approximate location of the area: Latitude: 26.7693 N, Longitude: 80.0282 W

Figure 3. Measurements used for model calibration

However, the noise floor value of -120dB is subtracted, and the spectrum scan is presented as the noise rise value in dB. The measurements are ordered top to bottom. In other words, the measurements collected around the green star (c.f. Fig. 3) are at the top of the Fig. 4, while the measurements collected around the red star (c.f. Fig. 3) are at the bottom of Fig. 4. There are more than 50,000 spectrum scans. Following observations may be made:

- The noise in the band is dominated by the three Wi-Fi channels (Channel 1 – center frequency 2412MHz, Channel 6 – center frequency 2437MHz, and Channel 11 -center frequency 2462MHz). Other Wi-Fi channels are used as well, but to a lesser extent.
- In general, Wi-Fi seems to be the dominant source of the interference. In Fig. 4, one may easily identify Wi-Fi channels. The center frequencies of the Wi-Fi channels align with dark blue vertical lines of the spectrogram [4].
- The portion of spectrum between 2473 and 2483.5MHz appears to be unoccupied. Wi-Fi Channel 11 ends at 2473MHz [4]. The spectrum between 2473 and 2483.5MHz belongs to Wi-Fi Channels 12 and 13. It seems that on land, these channels are deployed infrequently and hence, the noise rise in the corresponding portion of the spectrum is considerably smaller than within the rest of the band.

- The largest noise rise is experienced in Channel 6 (2426-2448MHz). This channel is assumed as the channel with the worst-case noise rise.
- As expected, the noise rise depends on the distance between the measurement point and the coastal population on the land. The bright yellow parts of the trace in Fig. 3 occur in the vicinity of the Palm Beach Shores and Singer Island which are well known destinations with many residences, hotels, and high-rises. Wi-Fi access points, and other ISM devices deployed throughout these two areas create a substantial noise rise within the band.

A set of traces for the noise rise in few Wi-Fi channels is presented in Fig. 5. One observes that the noise rise profile in channels 1, 6 and 11 is quite similar. Channel 6 is somewhat noisier than the other two, but the differences are not that large. Channel 13 is at the edge of the ISM band and its noise rise is 3-4dB lower than what is recorded in Channel 1. However, this cannot be attributed to a deployment of Channel 13 devices. The overlap between Wi-Fi channels is very large, and Channel 11 and 13 share the spectrum between 2461MHz and 2473MHz (12MHz). The noise rise in Channel 13 is predominantly a result of the Channel 11 deployments. To clarify the case in point, Figure 5 shows the noise rise for the upper 10.5MHz of spectrum (2473-2483.5MHz).

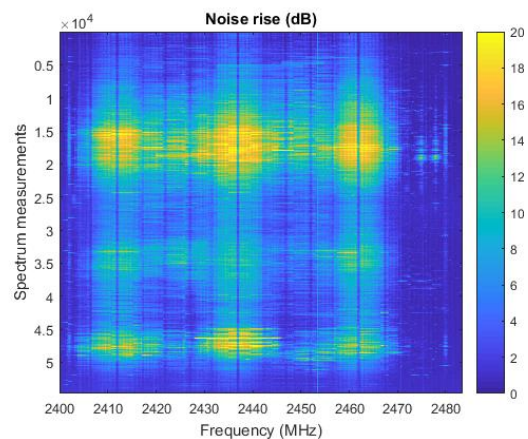


Figure 4. Noise rise spectrogram for the measurements in Fig. 3.

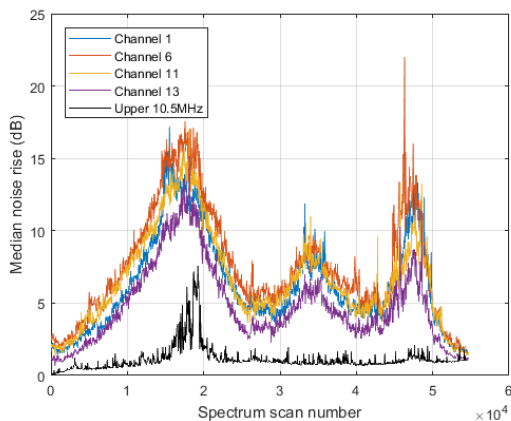


Figure 5. Comparison of the noise rise in different Wi-Fi Channels

One sees that for the most part, the noise rise in this portion of the spectrum stays way below 5dB.

IV. NOISE FLOOR MODELING

For the coastal waters, the most dominant source of the noise is the onshore deployment of the Wi-Fi systems. It is easy to understand that the density of such a deployment is fundamentally dependent on the population density. Therefore, the noise rise that one experiences in the coastal waters depends on the two factors: population density on the shore and the distance of the boat from the shore. On the basis of these observations, one may develop a simple model for the noise rise.

Consider the situation depicted in Fig. 6. The boat in the figure is traveling in the coastal waters. An element of the noise power within a given Wi-Fi channel that reaches the boat may be expressed as

$$dP_{NC} = K_c \frac{\rho(x, y)}{L(d)} dx \cdot dy \quad (1)$$

Where $\rho(x, y)$ is the population density at the elementary area (shaded square in Fig. 6), $L(d)$ is the path loss between the elementary area and the boat's receive antenna, d is the distance between the boat's antenna and elementary area, $dx \cdot dy$ is the size of the elementary area and K_c is the constant of proportionality. This constant depends on the channel since the occupancy of Wi-Fi channels is not uniform. As evident from Fig. 4, Channel 6 is the highest occupied channel. Channels 1 and 11 have high occupancy as well. Other channels have much lower occupancy.

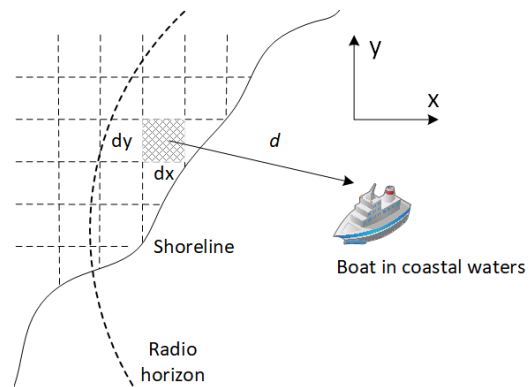


Figure 6. Noise floor modeling approach

The path loss model for the ISM band in the coastal waters is studied in [1]. Based on these studies, a nominal path loss model has a form of

$$L(d) = L_0 \times d^n \quad (2)$$

where L_0 is the median path loss between the source and the reference distance of 1km, d is the distance between the radiation source and the receiver and n is the path loss exponent.

According to [1], nominal value for median path loss to 1km is 101.7dB (i.e., 1.479×10^{10} in linear domain) and the nominal value for path loss exponent is 4.

By substituting (2) into (1), one obtains an estimate of the total noise power within a given Wi-Fi channel as:

$$P_{NC} = \iint_{(x,y) \text{ within radio horizon}} K_c \frac{\rho(x, y)}{L_0 d^n(x, y, x_0, y_0)} dx \cdot dy + N_0 \quad (3)$$

In (3) the location of the boat is (x_0, y_0) , and the function $d(x, y, x_0, y_0)$ represents the distance between the boat and an elementary area at the location (x, y) . The last term in (3), N_0 , is the thermal noise. Given the Wi-Fi bandwidth of 22MHz and the noise figure of 5dB, the value of the noise floor component is -95.6dBm (or 2.783×10^{-10} mW).

In general, the proportionality constant K_c is unknown. Within this paper, the value of K_c is determined from measured data using regression analysis. This process is referred to as the "model calibration". To understand the model calibration, consider a prediction of the noise within a Wi-Fi channel at the i th location. One may write

$$P_{NCpi} = K_c \cdot \iint_{R_n} \frac{\rho(x, y)}{L_0 d_i^n} dx \cdot dy + N_0 = K_c Z_{ni} + N_0 \quad (4)$$

In (4) the area of integration (R_n) is the radio horizon of the i th measurement location. To simplify the notation, the double integral is replaced with the symbol Z_{ni} . The function Z_{ni} depends on the location, and it is proportional to the noise created by the band's utilization on land. Let P_{NCmi} be the measurement of the noise power within the channel at the same i th location. Then the difference, between P_{NCmi} and P_{NCpi} represents the prediction error at the i th location. The Mean Square Error (MSE) across all locations may be written as:

$$MSE = \sum_{i=1}^N (K_c \cdot Z_{ni} + N_0 - P_{NCmi})^2 = F(K_c) \quad (5)$$

By minimizing $F(K_c)$ with respect to K_c , one obtains

$$K_c = \frac{\sum_{i=1}^N (P_{NCmi} - N_0) Z_{ni}}{\sum_{i=1}^N Z_{ni}^2} \quad (6)$$

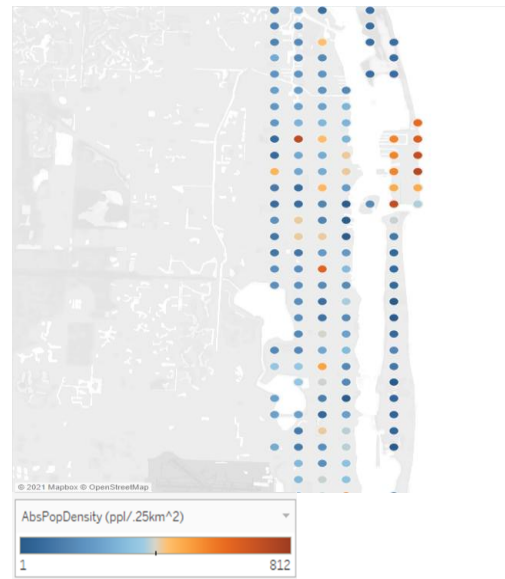
The value in (6) is a regression value for the Wi-F channel specific coefficient of proportionality.

V. CALIBRATION OF THE MODEL

For the purpose of model calibration, a population density map of the area is used. The map is displayed in **Fig. 7**. Each point on the map represents the population count in a square that is 500m on a side. As seen, the population counts vary from zero, over the waters and some small sections of the land, to 812 in some areas along the beach.

Utilizing the approach, outlined by (4)-(6), the coefficients of proportionality are obtained for all thirteen W-Fi channels in the ISM band. The results are summarized in Table 2. To illustrate the use of Table 2, consider the prediction model for Wi-Fi channel 6.

The prediction of the noise power at the i th location becomes



The color of each point indicates the number of people residing within a square that is 500m on a side.

Approximate location of the area: Latitude: 26.7693 N Longitude: 80.0282 W

Figure 7. Population density in the area impacting the noise floor measurements.

Table 2. Coefficient of proportionality (K_c)

Wi-Fi Channel	Frequency range [MHz]	K_c [mW (km) ⁿ⁻²]	St. dev. of prediction error [dB]
1	2401-2423	0.103	1.9
2	2406-2428	0.119	2.0
3	2411-2433	0.128	2.0
4	2416-2438	0.154	2.1
5	2421-2443	0.185	2.1
6	2426-2448	0.185	2.1
7	2431-2453	0.175	2.2
8	2436-2458	0.135	2.1
9	2441-2463	0.124	2.1
10	2446-2468	0.132	2.1
11	2451-2473	0.119	2.0
12	2456-2478	0.105	1.8
13	2461-2483	0.067	1.5

$$P_{N6pi} = 0.185 \text{ mW} \cdot \text{km}^2 \times \sum_{\substack{d < R_H \\ \text{and} \\ R_H < 3.7\sqrt{5} \text{ km}}} \frac{\rho(x, y) \cdot 0.25 \cdot \text{km}^2}{1.479 \times 10^{10} \cdot d^4} + 2.783 \times 10^{-10} \cdot \text{mW} \quad (7)$$

According to Table 2, for Wi-Fi channel 6, the proportionality constant is $K_c = 0.185 \text{ mW} \cdot \text{km}^{n-2}$.

The analysis in [1], report the path loss exponent of $n = 4$. Since the population density is available at the resolution of a 500m square bin, the integral in (3) becomes a summation. The value of $0.25 \cdot \text{km}^2$ is the size of the elementary surface $dx \cdot dy$. The radio horizon for a receiver that is 3m above the surface of the sea is given by $R_H = 3.7\sqrt{3}$ km [5]. The distance d in (7) is given in km. Finally, the value of $2.783 \times 10^{-10} \cdot \text{mW}$ is the thermal noise floor within 22 MHz Wi-Fi channel as observed by a receiver with a 5dB noise figure.

Using (7), predictions of the noise floor are obtained and compared against the measurements. The comparison is presented in Fig. 8. One may observe a relatively good agreement between the measurements (blue line) and predictions (red line). For the most part, the two curves track each other within couple of dBs. There are, however, a couple of locations where the difference is slightly larger. Some insight in why this may be the case is presented as follows.

First, one may notice large variations of the measured data around measurement mark $\sim 47,000$. The area where tests were performed had few larger boats with the on-board Wi-Fi systems. In few instances, these larger boats would be close to the measurement boat and their Wi-Fi would elevate the measured noise floor. One such instance occurs around measurement mark 47,000.

Figure 9 presents a section of the measurement trajectory colored by the absolute value of the prediction error for Wi-Fi Channel 6. One notices that the absolute difference becomes larger as the measurement boat comes closer to the shore. By its very nature, the model in (3) assumes that the Wi-Fi channel noise is an aggregation of small contributions from many access points. This is a very reasonable assumption when the boat operates in an area that is far from the shore.

However, when the boat approaches the shore, the fine details of the access points distribution on land become important. For example, around measurement mark 43,000 (section shown in Fig. 9), the measured noise floor is significantly lower than what is predicted.

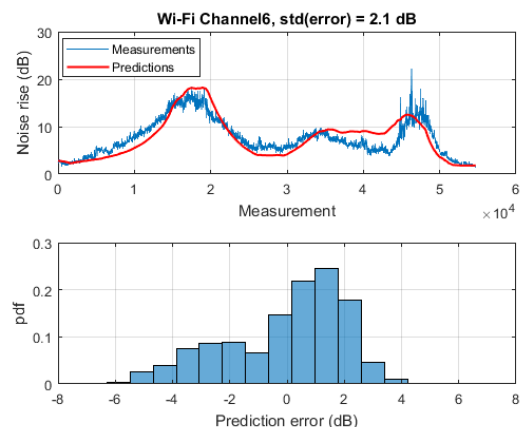


Figure 8. Comparison of measurements and predictions for Wi-Fi Channel 6 (Calibration data)



The color of the trace indicates absolute difference between measured noise floor and predicted noise floor expressed in dB.

Approximate location of the area: Latitude: 26.7632 N, Longitude: 80.0332 W

Figure 9. Location of significant differences between measurements and predictions

At this location, the boat is right in front of a golf-course which practically has no Wi-Fi access points, a construction site and a few larger estates that might have been unoccupied during the measurement campaign.

VI. VERIFICATION OF THE MODEL

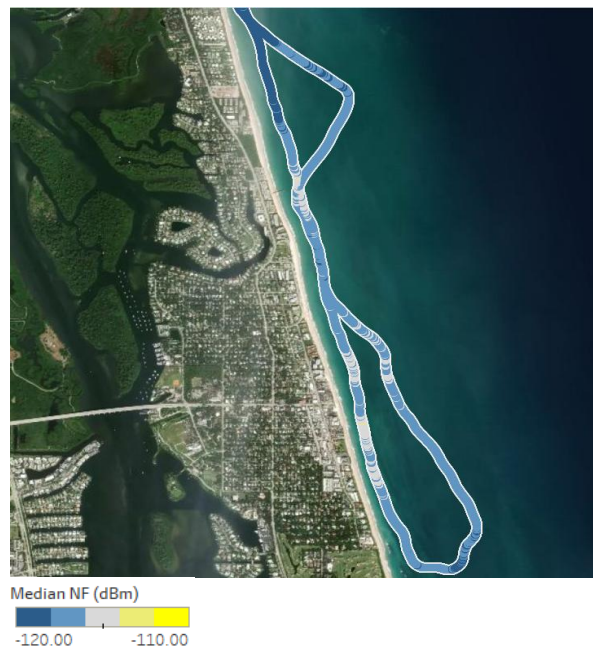
For the noise floor model verification and testing, a different coastal location is selected. A section of the cost between Sebastian and Vero Beach, FL is surveyed (c.f. Fig. 10). This area is not as heavily populated as the calibration area near West Palm Beach. The population density is close

to median population density along Florida's coast, and therefore this area may be considered as a more typical. The boat trajectory used for the measurements is presented in Fig. 10. One may observe that the trajectory is closer to the shore than in the case of West Palm Beach measurements (c.f. Fig.4). In Fig. 10, the color of the trace indicates median received power within 80kHz of the receiver's bandwidth. By comparing Figs 4 and 10, one immediately notices that the verification data exhibit a substantially smaller noise rise. This could be expected since the verification area has a smaller population density.

To further illustrate the point, the spectrogram associated with the measurements in Fig. 10 is presented in Fig. 11. Just as in the case of West Palm Beach measurements, one may clearly identify Wi-Fi channels. They represent dominant sources of the noise rise in the band. Most of the noise is noticed on channels 1, 6 and 11, with Channel 11 having the highest noise rise. This is different from what was observed in the calibration data (c.f. Fig. 4) where Channel 6 has the largest amount of noise. One may expect slight variations in the distribution of the deployment between primary channels (1,6 and 11) from location to location. Hence, the coefficients in Table 2 may change somewhat between different geographical locations. For preliminary considerations, a notion of the "noisiest Wi Fi channel" (nWi-Fi) is introduced.

The nWi-Fi is the channel that has the highest noise rise. All other channels at a given location have the noise rise that is smaller than nWi-Fi. In the case of calibration data, the noisiest channel is Channel 6. In the case of verification data, the noisiest channel is Channel 11. For the noise rise prediction model in (3), it is assumed that

the nWi-Fi has $K_c = 0.185 \text{ mW} \cdot \text{km}^{n-2}$. Equation (7) is used for prediction of the noise rise within Channel 11 of the measurements in Fig. 10. As seen in Fig. 11, Channel 11 is the nWi-Fi for the verification area. The comparison between measurements and model predictions is presented in Fig. 12. The following observations may be made:



The color of the trace indicates median noise power across the band. The power is measured within a bandwidth of 80 kHz. (c.f. Table 1). The color bands are slightly different than Fig. 3. The noise floor in this case is much lower as there are no high-density population areas.

Approximate location of the area: Latitude: 27.6624 N, Longitude: 80.3554 W

Figure 10. Location of the measurements used for model verification

- There is a good agreement between the measurements and predictions. The mean difference between the two is smaller than 3dB and the standard deviation of the prediction error is 2.9dB.
- The prediction model tends to overestimate the noise rise. One possible explanation is in that model does not consider the heights of the access points on the shore. For the calibration area, many of the Wi-Fi access points are located on the higher floors of high-rise buildings. Signals emitted from higher radiation centerlines tend to propagate further [5]. When the model is used in an area where the Wi-Fi access are closer to the ground it tends to overestimate the propagation distances of the signals.
- The trajectory of the boat during the verification measurement is close to the shore. By its very nature, the model assumes that the noise is a result of signal aggregation from many small sources. In the vicinity of the shore, this may not be the case and the noise rise may be

dominated by few sources that are close to the coastline.

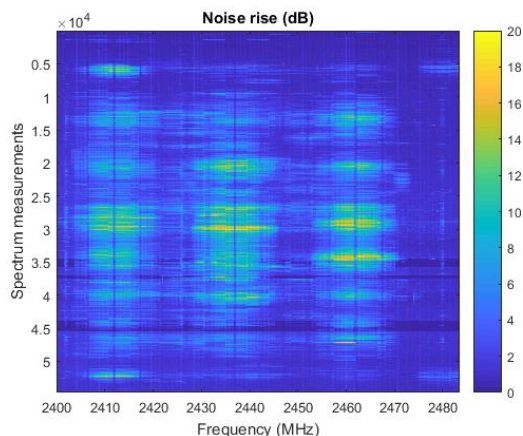


Figure 11. Spectrogram for the measurements in Fig. 10.

As a final observation, one notes that the upper 10.5MHz in Fig. 11 (2473-2483.5MHz) seem to be free from any significant activity. This is consistent with the spectrogram of calibration measurements presented in Fig. 4.

VII. SUMMARY AND CONCLUSIONS

This paper presents a measurement campaign for characterizing the noise floor within the 2.4GHz ISM band, as it is observed within the coastal waters of Florida. It was established that the noise floor rise depends largely on Wi-Fi deployment on the shore. As such, the rise in the noise floor is closely correlated with the population density of the area. Based on this observation, a simple noise floor model is developed.

The model predicts the noise rise as a function of the population density. Using measurements collected at two different costal locations, the model is calibrated, and its accuracy is accessed and verified. It is observed that the model could be improved by including the heights of the man-made structures in the modeling process. Also, further testing of the model under various coastal morphologies should be conducted.

The measured data uncovered that the spectrum between 2473 and 2483.5MHz has almost no utilization.

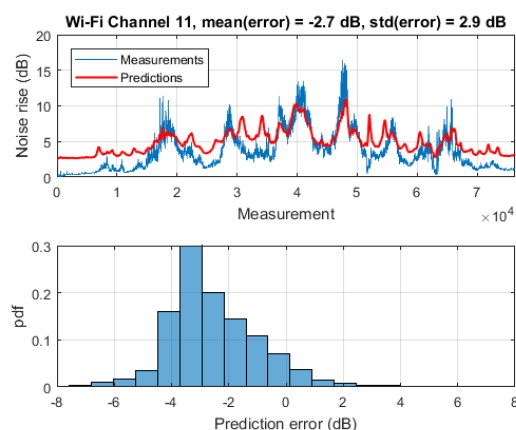


Figure 12. Comparison of measurements and predictions for Wi-Fi Channel 11 (Verification data)

Therefore, this portion of the ISM band could be used for development of a short-range communication network for connectivity of the boats within coastal waters. A possible approach could be to use this spectrum for a primary channel. This channel would be mostly interference free. The rest of the ISM spectrum may be used opportunistically for supplementary data channels.

ACKNOWLEDGEMENTS

The author would like to acknowledge Mr. Zachary Naylor and Gabe's Wireless Solutions for providing help with the measurement equipment and data collection.

REFERENCES

- [1]. R. Enaya and I. Kostanic, "Over the Ocean RF Propagation Modeling and Characterization," *International Journal of Engineering Research and Applications (IJERA)*, Vol. 10, No. 11, November 2020.
- [2]. – Code of Federal Regulations, Title 47, Part 15, https://www.ecfr.gov/cgi-bin/text-idx?c=ecfr&tpl=/ecfrbrowse/Title47/47cfrv1_02.tpl, accessed January 2021.
- [3]. – PCTEL, Seagull scanning receiver, <https://www.pctel.com/products/test-measurement/scanning-receivers/>, accessed January 2021.
- [4]. B. O'Hara and A. Petrick, *IEEE 802.11 Handbook, A designer's Companion, 2nd Ed.* IEEE Press, 2005.
- [5]. J. F. Parsons, *The Mobile Radio Propagation Channel, 2nd Ed.*, John Wiley and Sons, 2001.